

REHABILITATION ROBOT CONFIGURATIONS FOR WALKING

Chapter – 7

REHABILITATION ROBOT CONFIGURATIONS FOR WALKING

7.1 INTRODUCTION

Using the dynamic motion optimization technique, four different configurations were studied:

- **Configuration-1:** Paralyzed swing leg with motion captured stance hip orientation (no optimization). This configuration was studied to determine if simply applying a normative pelvis trajectory would effectively control the swing leg.
- **Configuration-2:** Unimpaired swing leg with effort minimization of all joints. This configuration was studied to determine if the optimization technique produced a realistic gait trajectory if the leg was fully actuated.
- **Configuration-3:** Paralyzed swing leg with effort minimization of the stance hip torques. This configuration was studied to determine to what extent swing of a paralyzed leg could be controlled with pelvis motion.
- **Configuration-4:** Paralyzed swing leg with effort minimization of the stance hip torques and bounded stance hip orientation.

For these simulations, the stance and swing legs were the left and right legs, respectively. The stance hip joint center locations for different walking speeds were approximated by B-spline curves based on the motion capture data. Different weighting coefficients and different z_1 and z_2 for avoiding the collision of the legs were used in the optimization. The results corresponding to the different walking speeds for each configuration are discussed. The optimization results are represented as solid lines, and the actual human gait as dashed lines for comparison.

7.2 PARALYZED SWING LEG WITH MOTION CAPTURED STANCE HIP ORIENTATION (Configuration -1)

No optimization was applied in this configuration, in order to determine how the leg would swing if the pelvis were simply moved in a normative trajectory. The swing hip,

knee and ankle joints were set to be passive while the stance hip joint followed the trajectory identified from motion capture. Assuming no ground contact, the equations of motion were solved and the resulting motions are shown in Figure 7.1.

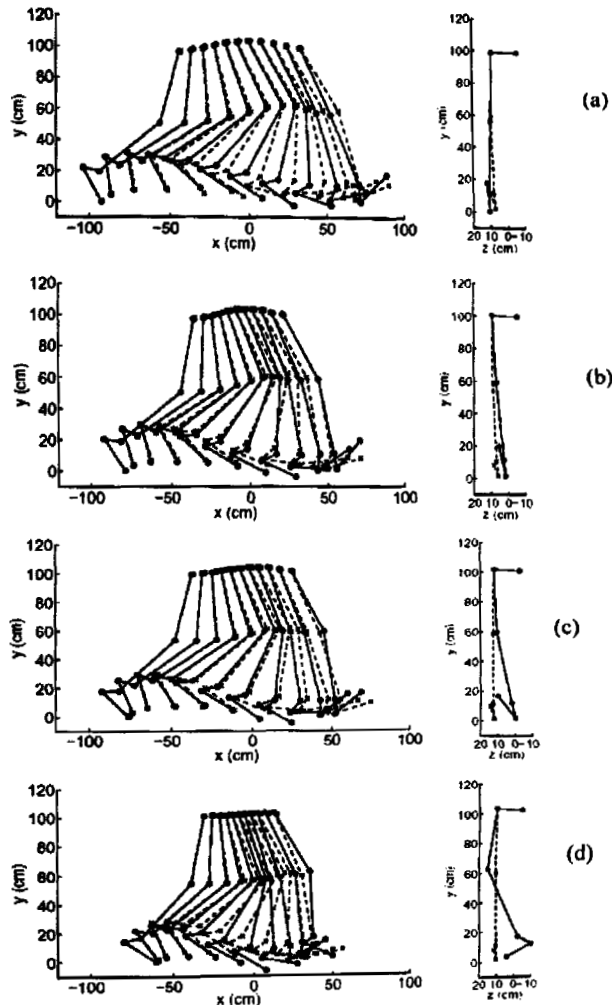


Figure 7.1. The resulting gait for configuration-1. The solid lines show the resulting gait and the dashed lines are the gait recorded from the motion capture system). (a) duration 0.43 sec. (b) duration 0.47 sec, (c) duration 0.50 sec, and (d) duration 0.57 sec

Figure 7.1 shows that the swing leg moves at its natural frequency. However, there would be a collision between the leg and the ground at about $x = 0$ (mid-stride) if the ground were not neglected. Note also that the leg is internally rotated away from the desired configuration at the end of swing.

7.3 UNIMPAIRED SWING LEG WITH EFFORT MINIMIZATION OF ALL JOINTS (Configuration -2)

56 parameters (8 for each active joint) were used in the optimization. The parameters that set the limits on allowable out of plane motion of the legs, z_1 and z_2 in the penalty function J_{p2} , were chosen as

$$z_1(t) = z_{\text{stance hip}}(t) + l_{\text{hip}} - 0.005 \quad (7.1)$$

$$z_2(t) = z_{\text{stance hip}}(t) + l_{\text{hip}} - 0.033 \quad (7.2)$$

where " $l_{\text{hip}} - 0.005$ " and " $l_{\text{hip}} - 0.033$ " are the smallest distances between the swing knee and the stance hip and between the swing heel and the stance hip, respectively, identified from motion capture.

The weighting coefficients are listed in Table-7.1 and were chosen heuristically based on many simulations. The optimization was obtained in 4 hours with a Pentium II-700 MHz PC.

Table-7.1: Weighting coefficients in configuration-2

$w_{e4}, w_{e4}, \dots, w_{e8}$	w_{e9}	w_{e10}	w_{p1}	w_{p2}
0.05	0.10	2.50	5×10^5	5×10^5

The resulting gaits, joint positions and joint torques are shown in Figures 7.2–7.10. The good correspondence with the human data is consistent with previous studies that suggest that human gait involves the minimization of effort/energy [71]. This effort/energy is applied to lift swing leg to avoid the ground contact in addition to achieve the final configuration. Moreover, the correspondence between the optimized and actual joint motions suggest that the simulation can adequately predict what a normative trajectory would be, given only the limb dynamics and desired final configurations of the leg.

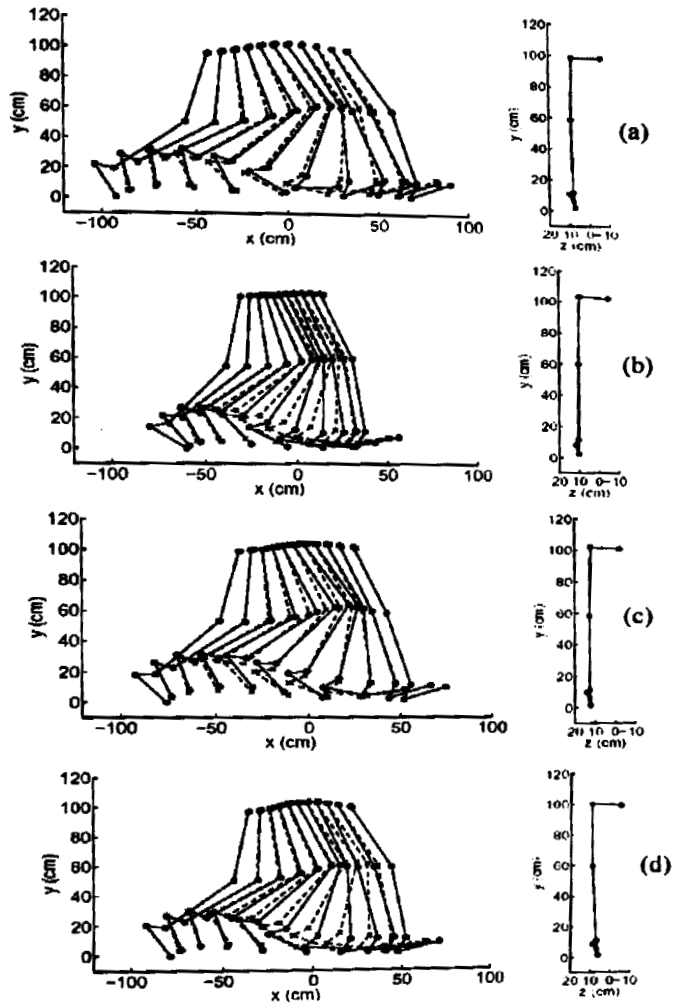


Figure 7.2. The resulting gait for configuration-2. The solid lines show the resulting gait and the dashed lines are the gait recorded from the motion capture system.) (a) duration 0.43 sec (b) duration 0.47 sec (c) duration 0.50 sec (d) duration 0.57 sec

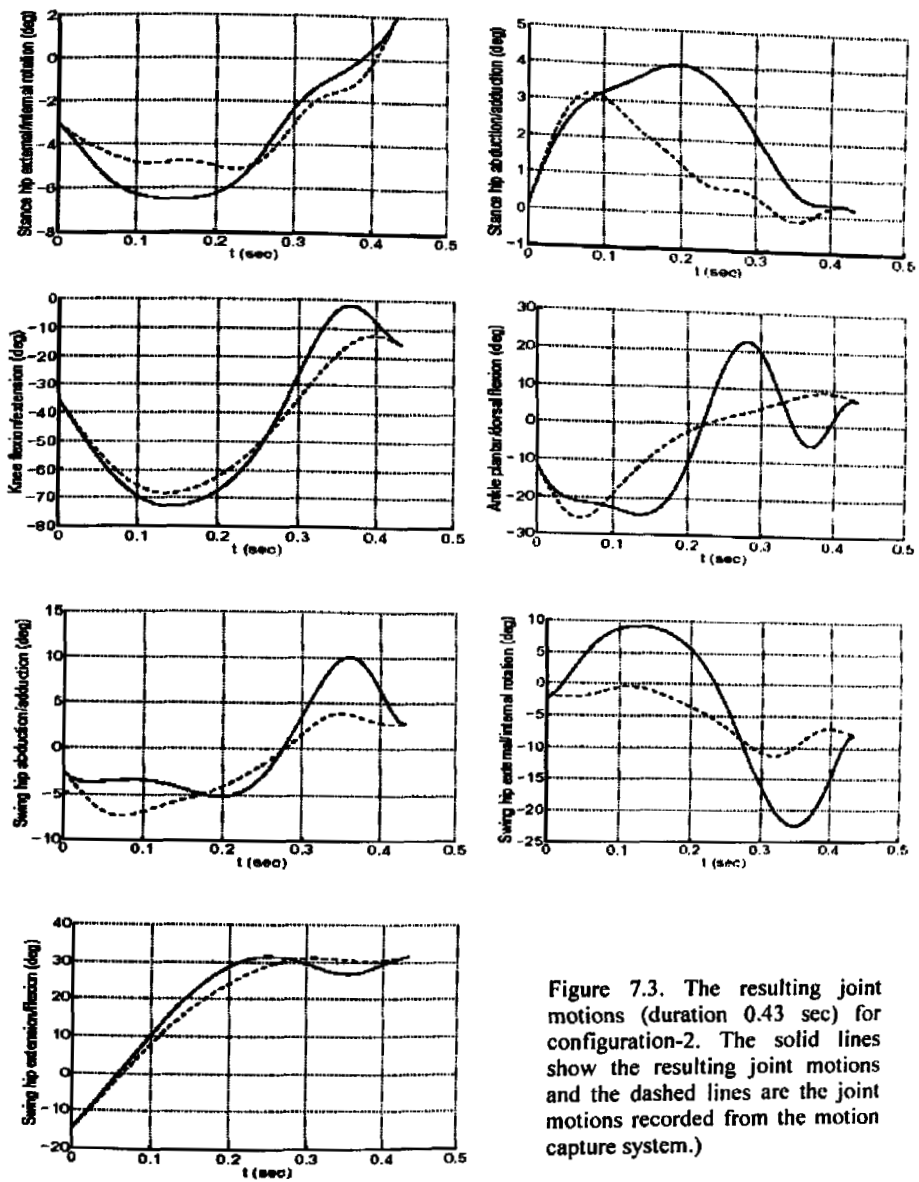


Figure 7.3. The resulting joint motions (duration 0.43 sec) for configuration-2. The solid lines show the resulting joint motions and the dashed lines are the joint motions recorded from the motion capture system.)

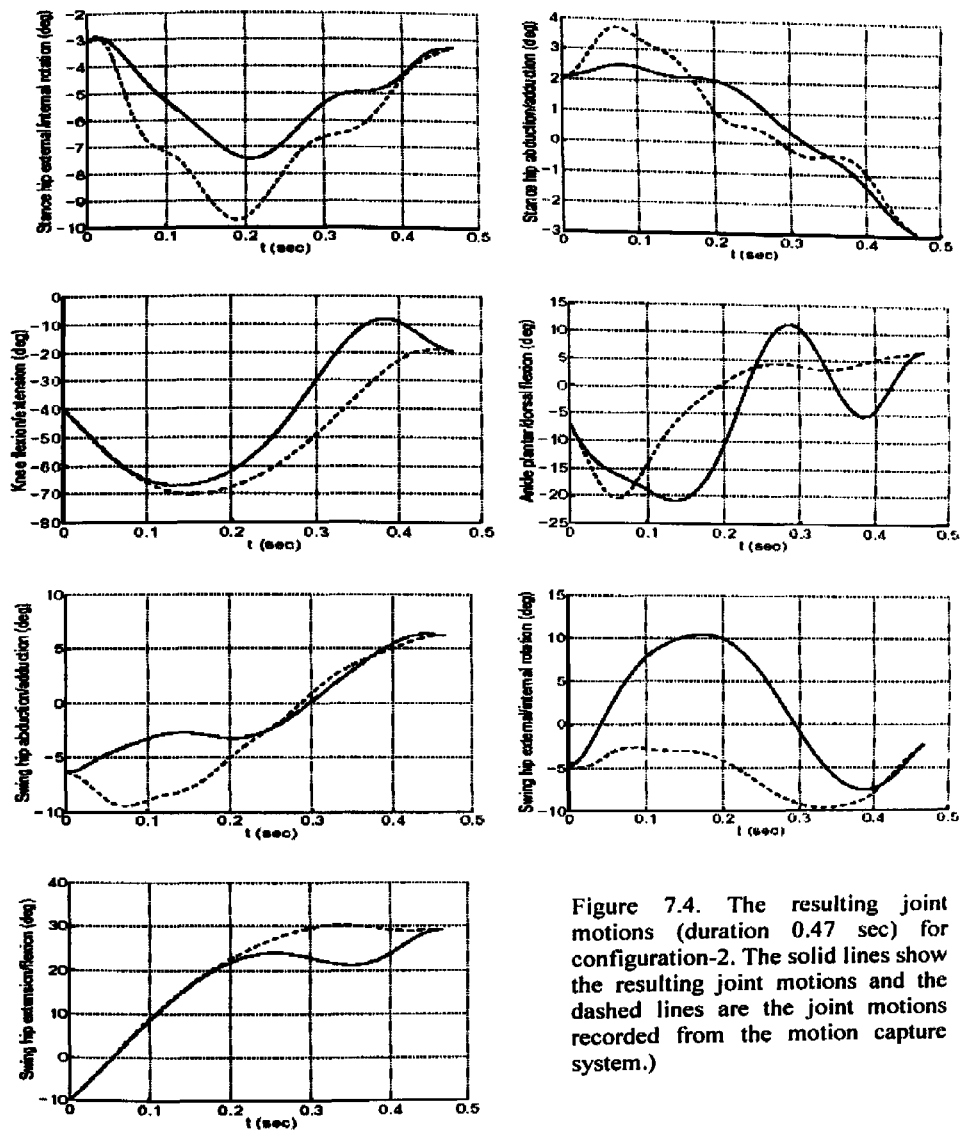


Figure 7.4. The resulting joint motions (duration 0.47 sec) for configuration-2. The solid lines show the resulting joint motions and the dashed lines are the joint motions recorded from the motion capture system.)

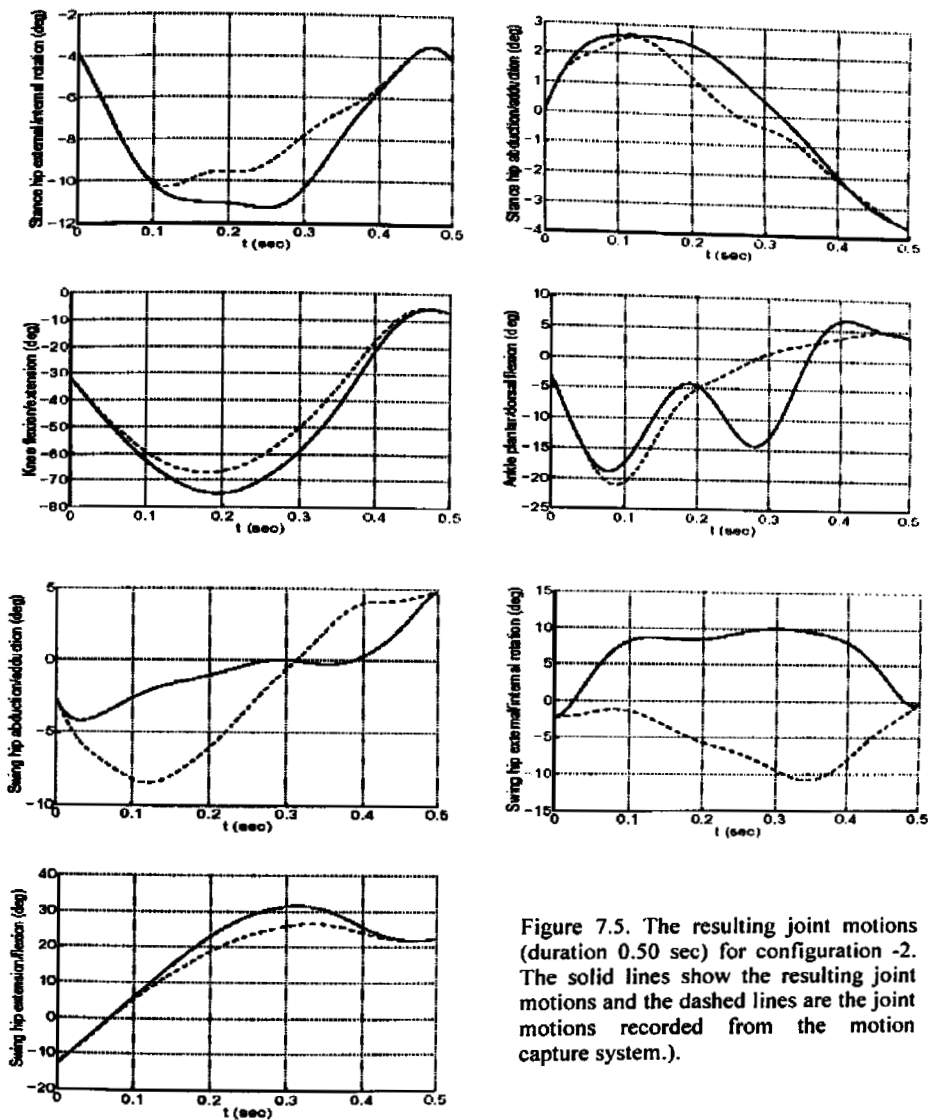


Figure 7.5. The resulting joint motions (duration 0.50 sec) for configuration -2. The solid lines show the resulting joint motions and the dashed lines are the joint motions recorded from the motion capture system.).

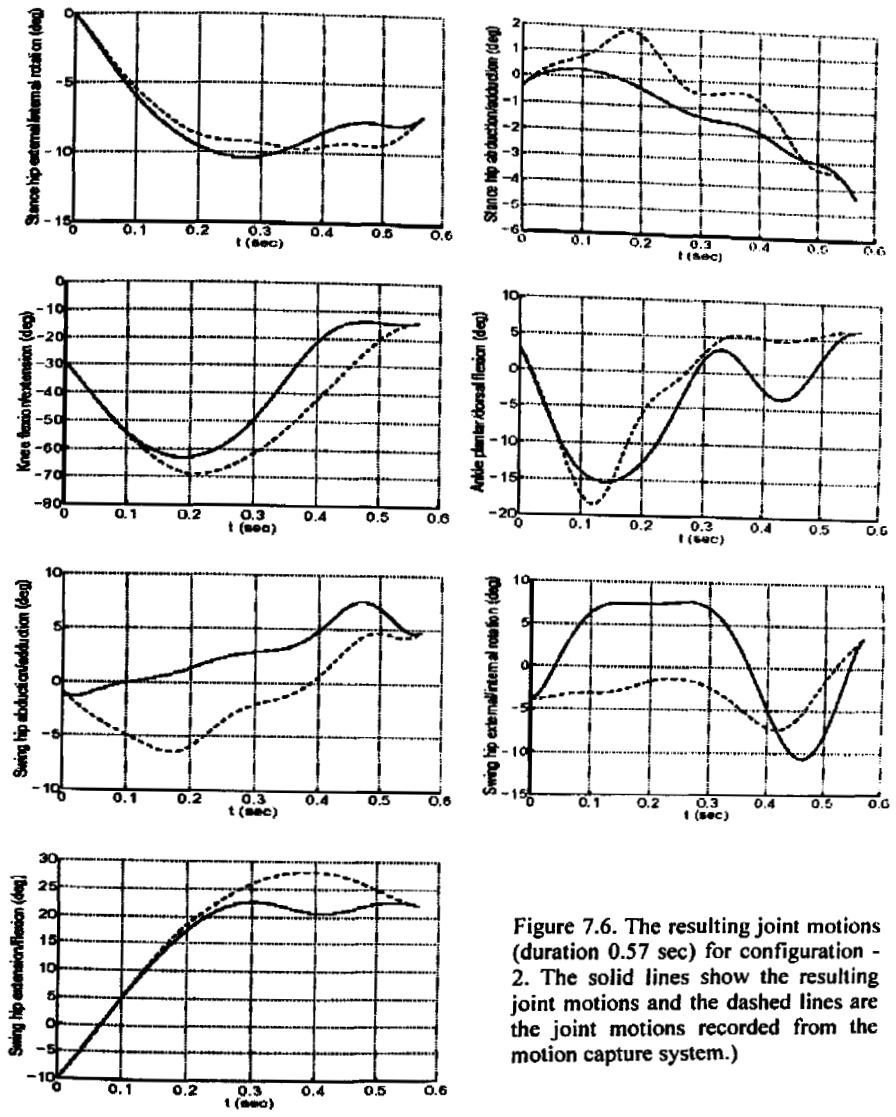


Figure 7.6. The resulting joint motions (duration 0.57 sec) for configuration - 2. The solid lines show the resulting joint motions and the dashed lines are the joint motions recorded from the motion capture system.)

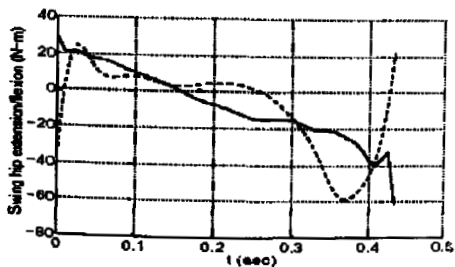
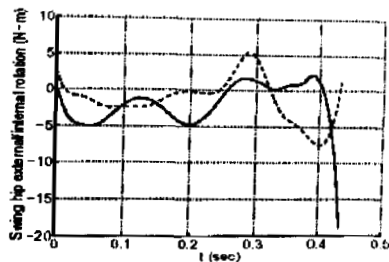
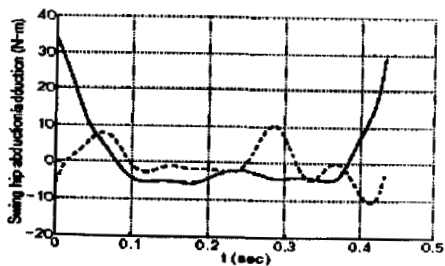
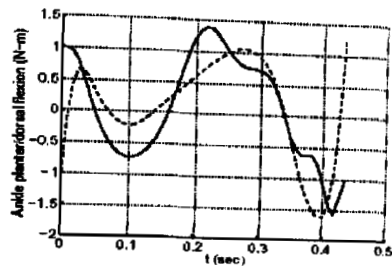
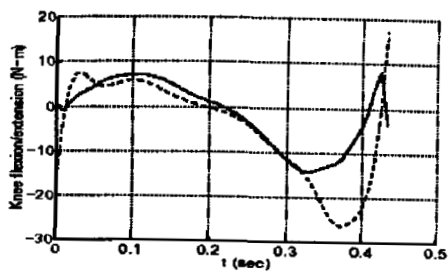
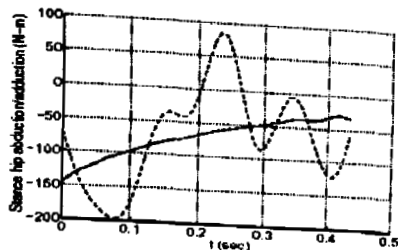
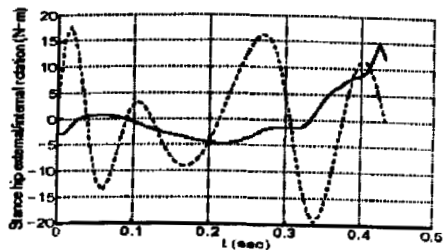


Figure 7.7. The resulting joint torques (duration 0.43 sec) for configuration-2. The solid lines show the resulting joint torques and the dashed lines are the joint torques corresponding to the motion capture data.)

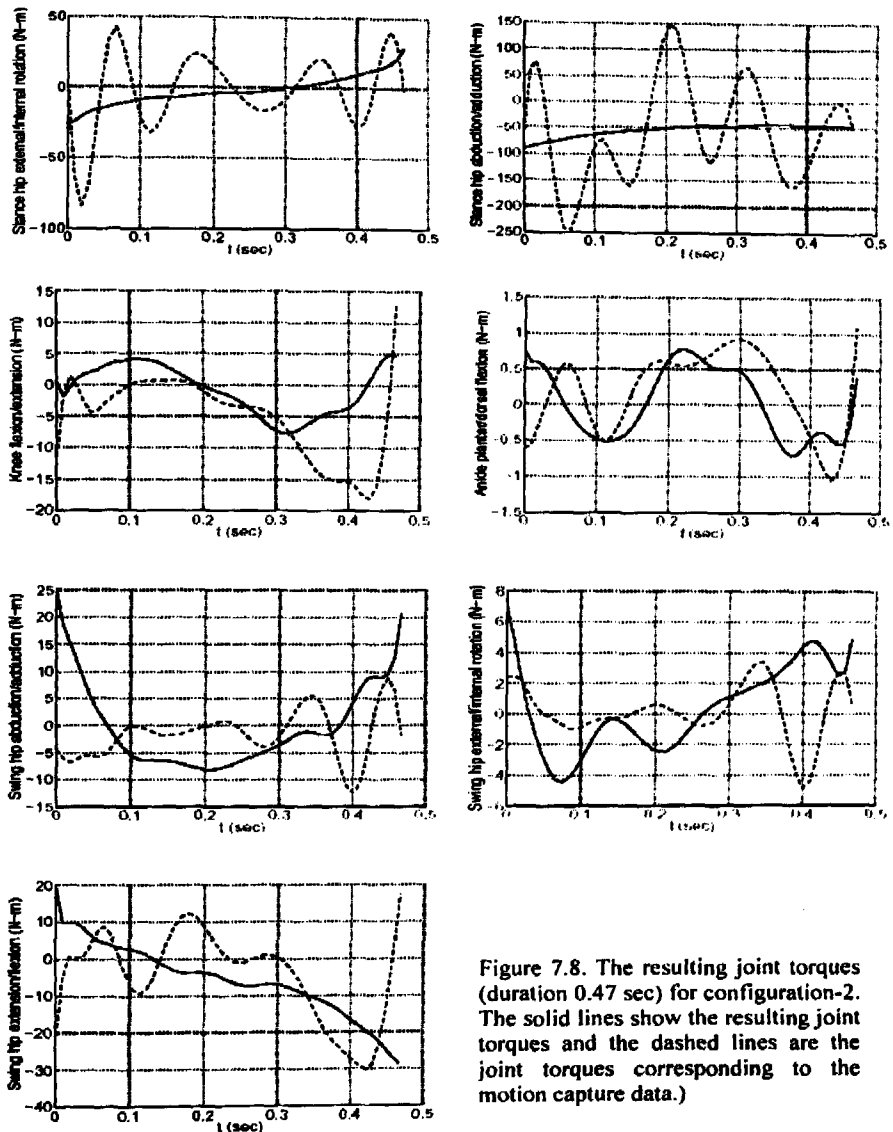


Figure 7.8. The resulting joint torques (duration 0.47 sec) for configuration-2. The solid lines show the resulting joint torques and the dashed lines are the joint torques corresponding to the motion capture data.)

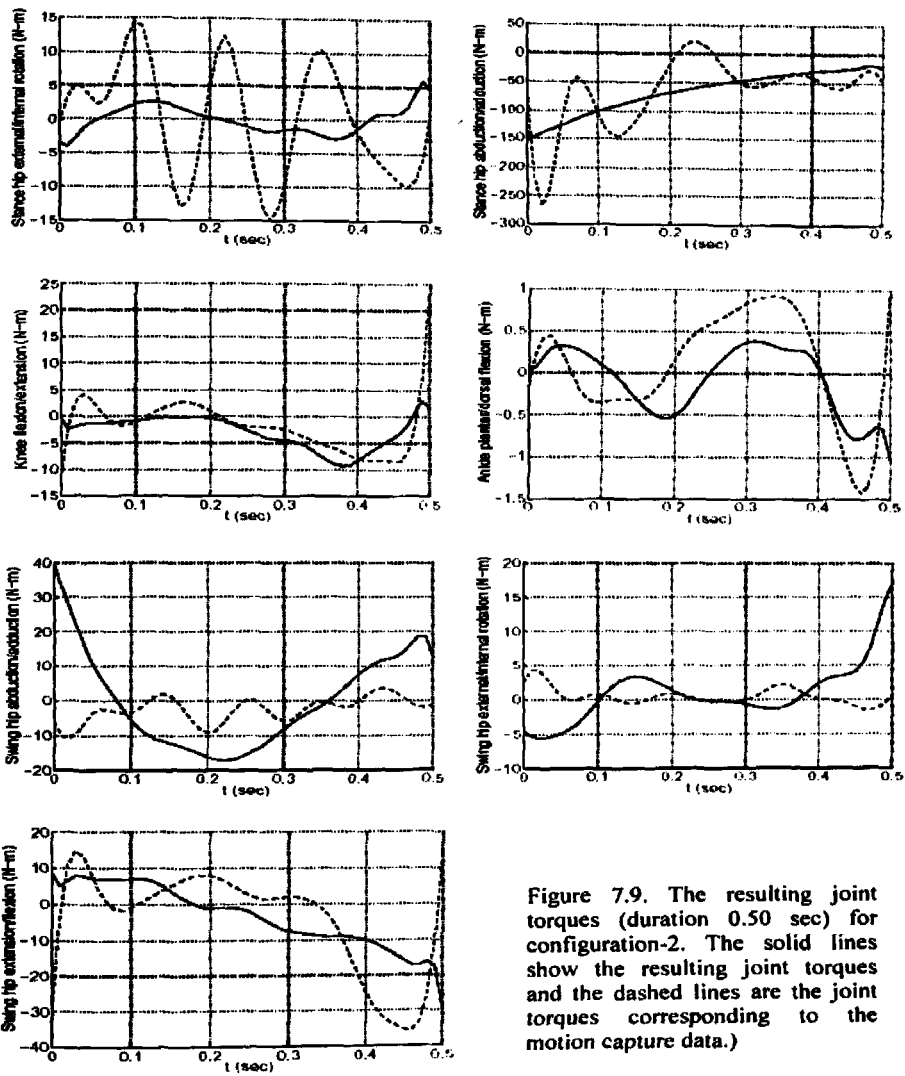


Figure 7.9. The resulting joint torques (duration 0.50 sec) for configuration-2. The solid lines show the resulting joint torques and the dashed lines are the joint torques corresponding to the motion capture data.)

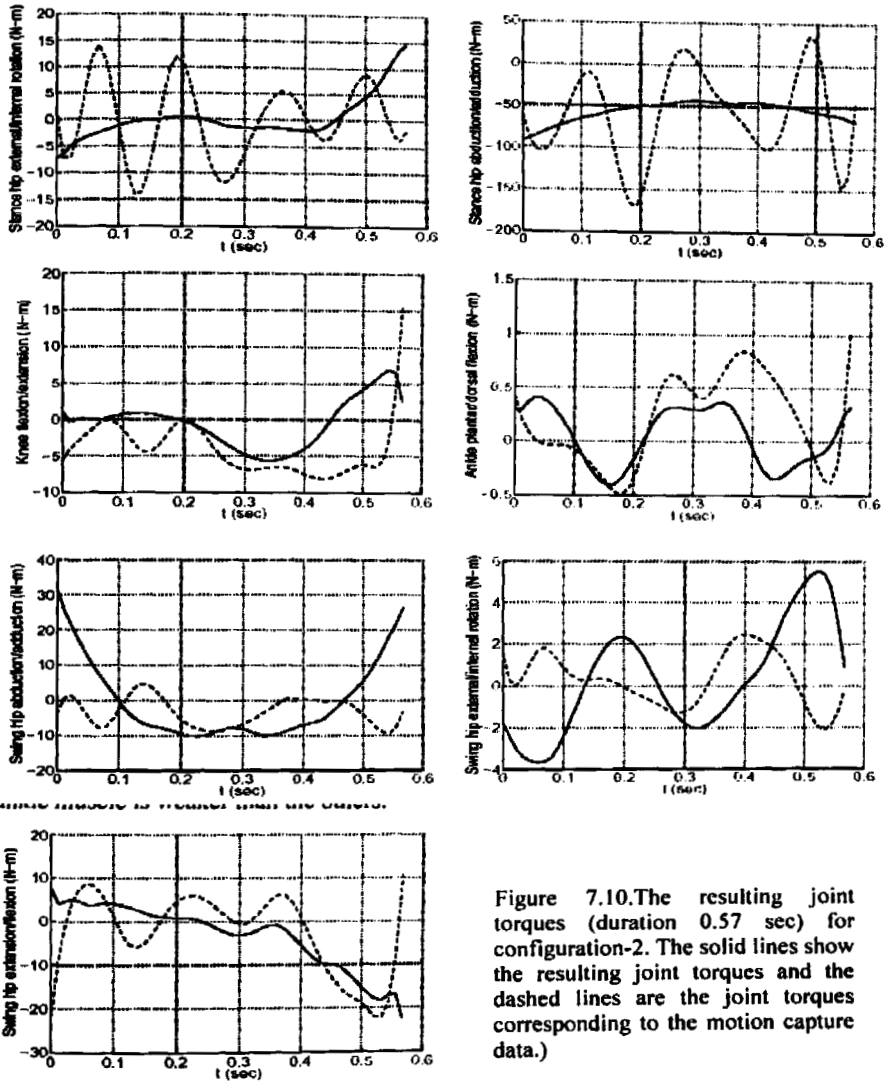


Figure 7.10. The resulting joint torques (duration 0.57 sec) for configuration-2. The solid lines show the resulting joint torques and the dashed lines are the joint torques corresponding to the motion capture data.)

Because the muscles interacting with the different joints have different strengths, different weighting coefficients, w_{ei} 's, were chosen for different joints. w_{e10} was larger than the rest of w_{ei} 's which restricts the ankle joint to use less applied torque and/or effort since the ankle muscle is weaker than the others.

7.4 PARALYZED SWING LEG WITH EFFORT MINIMIZATION OF THE STANCE HIP TORQUES (Configuration-3)

To simulate a paralyzed person, the swing hip, knee and ankle joints were made passive. 16 parameters (8 for each active joint) were used in the optimization. Although less parameters are used in this configuration than in the fully actuated configuration, the computation load for integration of the dynamics motion is actually higher. This is because the dynamics are hybrid with both active and passive joints, which the previous configuration had only active joints. The optimization took approximately 3 hours to complete.

The positions z_1 and z_2 in the penalty function J_{p2} were chosen as

$$z_1(t) = z_2(t) = z_{\text{stance hip}}(t) + \frac{2}{3}l_{\text{hip}} \quad (7.3)$$

which allows more hip adduction than the previous case. The weighting coefficients are listed in Table -7.2.

Table-7.2: Weighting coefficients in configuration -3

w_{e4}	w_{e5}	w_{p1}	w_{p2}	w_{p31}	w_{p32}
10^{-4}	10^{-4}	10^5	10^4	10^3	10^2

The results are shown in Figures 7.11–7.16. The optimizer lifted the swing hip to avoid the collision between the legs and between the swing leg and the ground. At the same time, it twisted the pelvis to pump energy into the paralyzed leg and moved the leg close to the desired final configuration. Thus the optimizer was able to determine a strategy that could achieve repetitive stepping by shifting the pelvis alone. Note that the strategy incorporated a large swivel by the stance hip joint around the y -axis that may be undesirable in step training a real human.

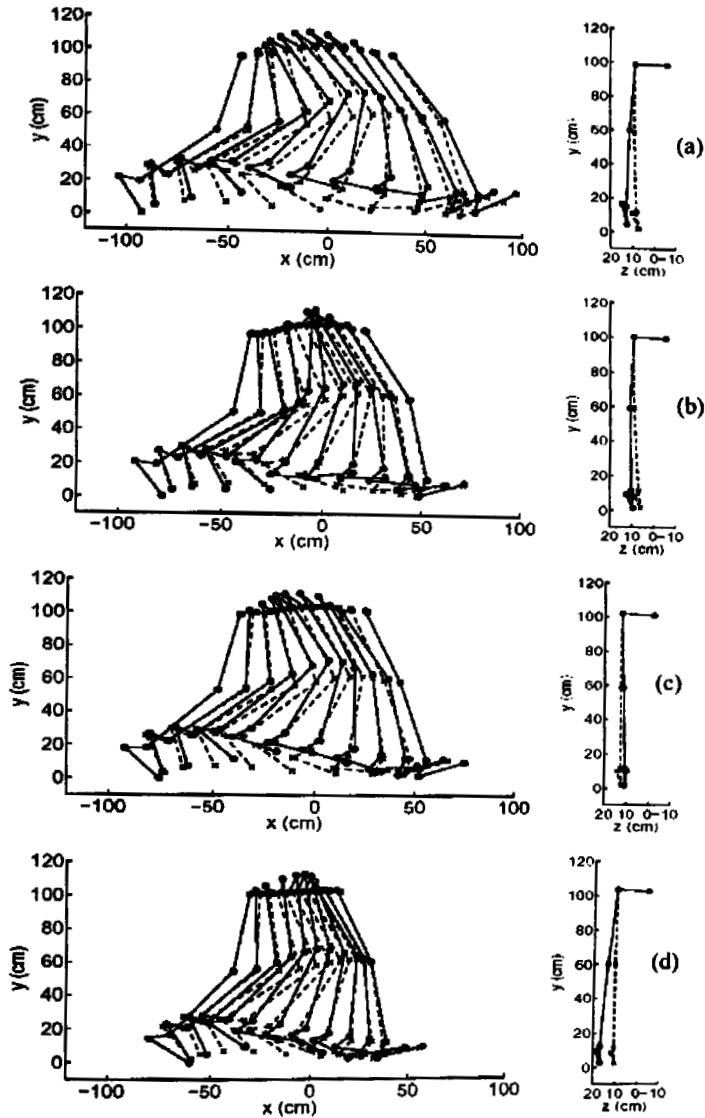


Figure 7.11. The resulting gait for configuration-3. The solid lines show the resulting gait and the dashed lines are the gait recorded from the motion capture system.) (a) duration 0.43 sec (b) duration 0.47 sec (c) duration 0.50 sec (d) duration 0.57 sec

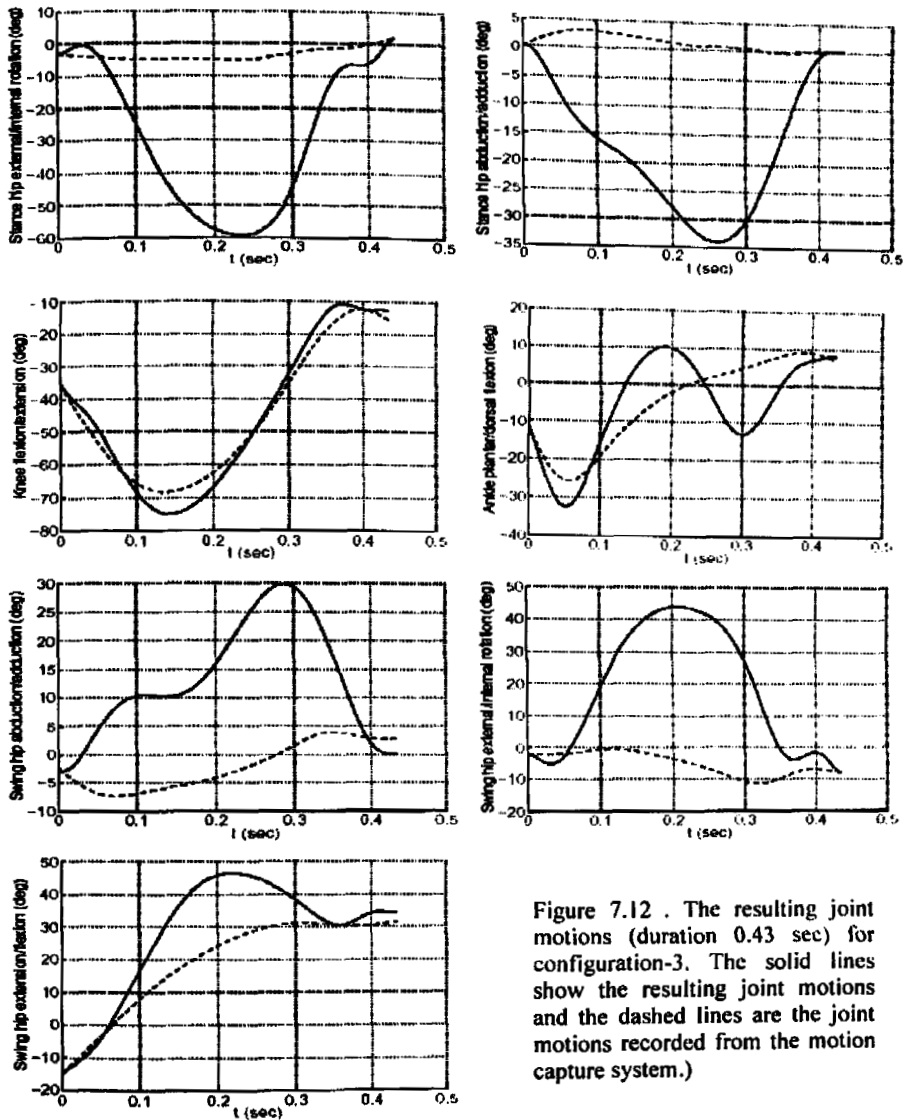


Figure 7.12 . The resulting joint motions (duration 0.43 sec) for configuration-3. The solid lines show the resulting joint motions and the dashed lines are the joint motions recorded from the motion capture system.)

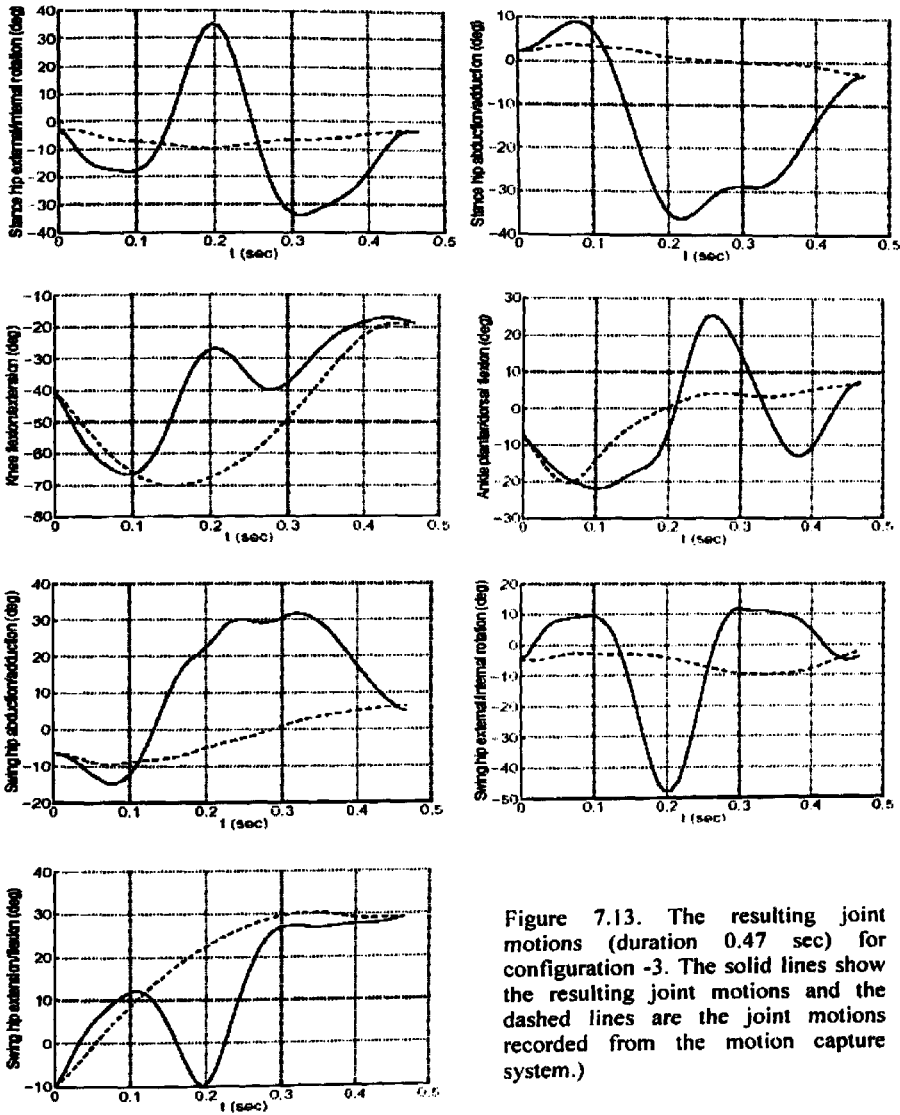


Figure 7.13. The resulting joint motions (duration 0.47 sec) for configuration -3. The solid lines show the resulting joint motions and the dashed lines are the joint motions recorded from the motion capture system.)

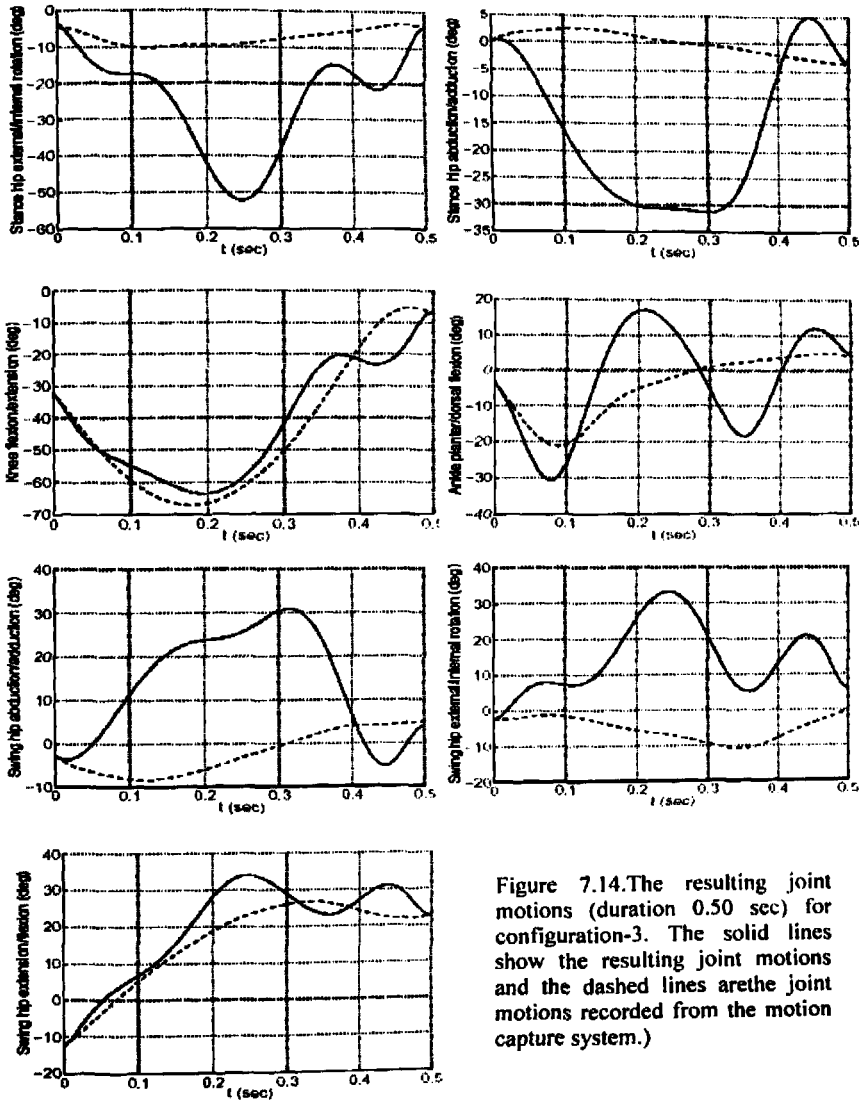


Figure 7.14. The resulting joint motions (duration 0.50 sec) for configuration-3. The solid lines show the resulting joint motions and the dashed lines are the joint motions recorded from the motion capture system.)

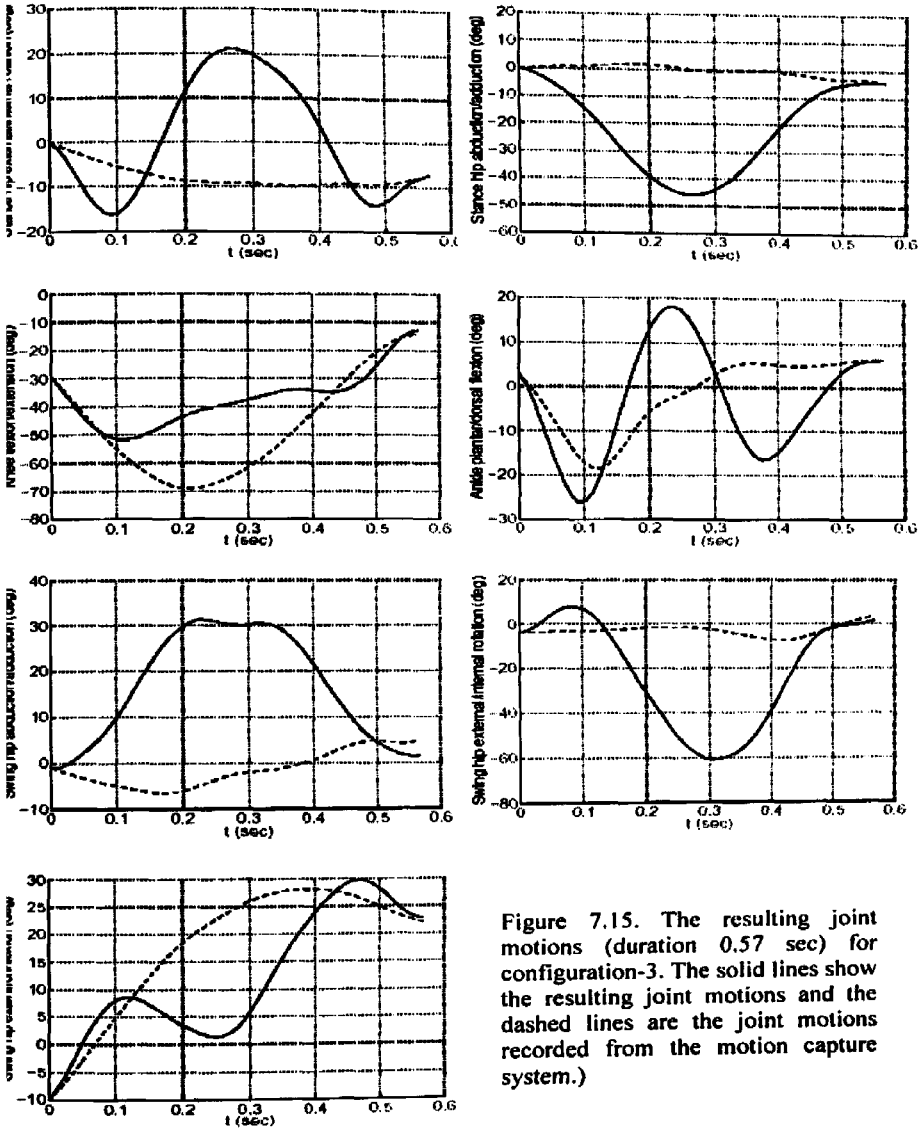


Figure 7.15. The resulting joint motions (duration 0.57 sec) for configuration-3. The solid lines show the resulting joint motions and the dashed lines are the joint motions recorded from the motion capture system.)

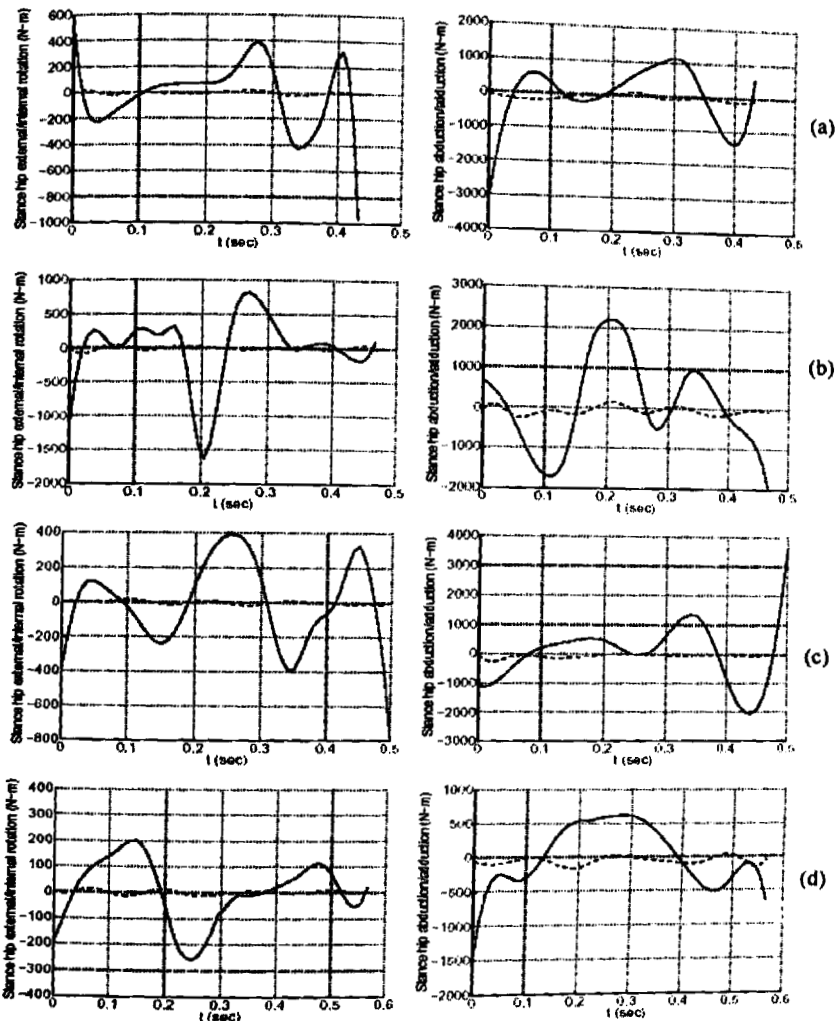


Figure 7.16. The resulting joint torques for configuration -3. The solid lines how the resulting joint torques and the dashed lines are the joint torques corresponding to the motion capture data.). (a) duration 0.43 sec (b) duration 0.47 sec(c) duration 0.50 sec (d) duration 0.57 sec

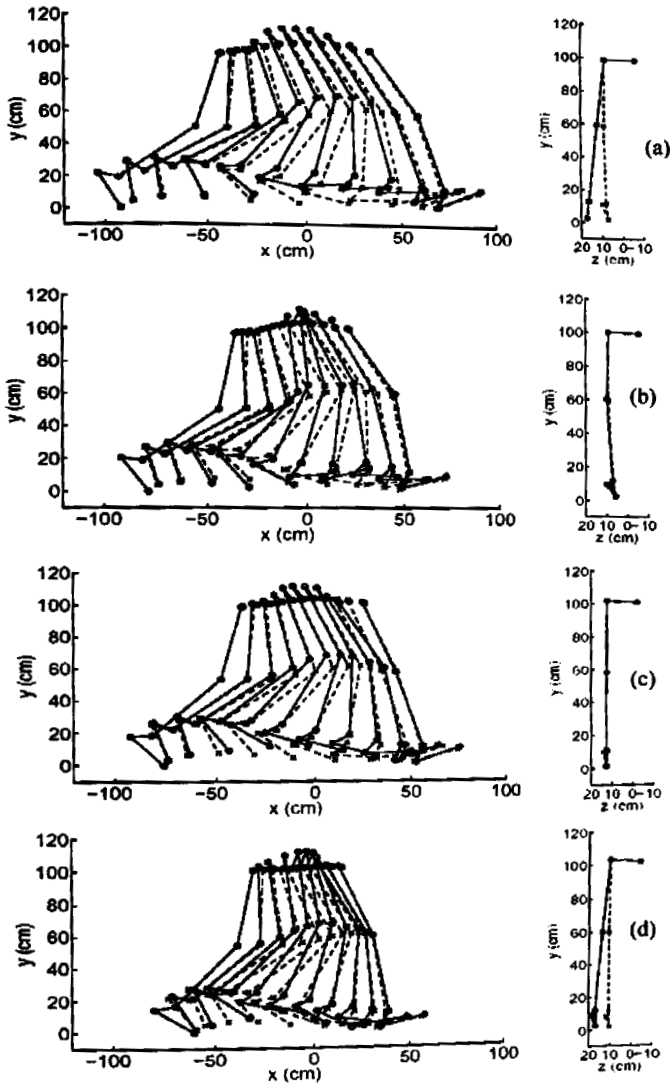


Figure 7.17 The resulting gait for configuration-4. The solid lines show the resulting gait and the dashed lines are the gait recorded from the motion capture system.) (a) duration 0.43 sec (b) duration 0.47 sec (c) duration 0.50 sec and (d) duration 0.57 sec

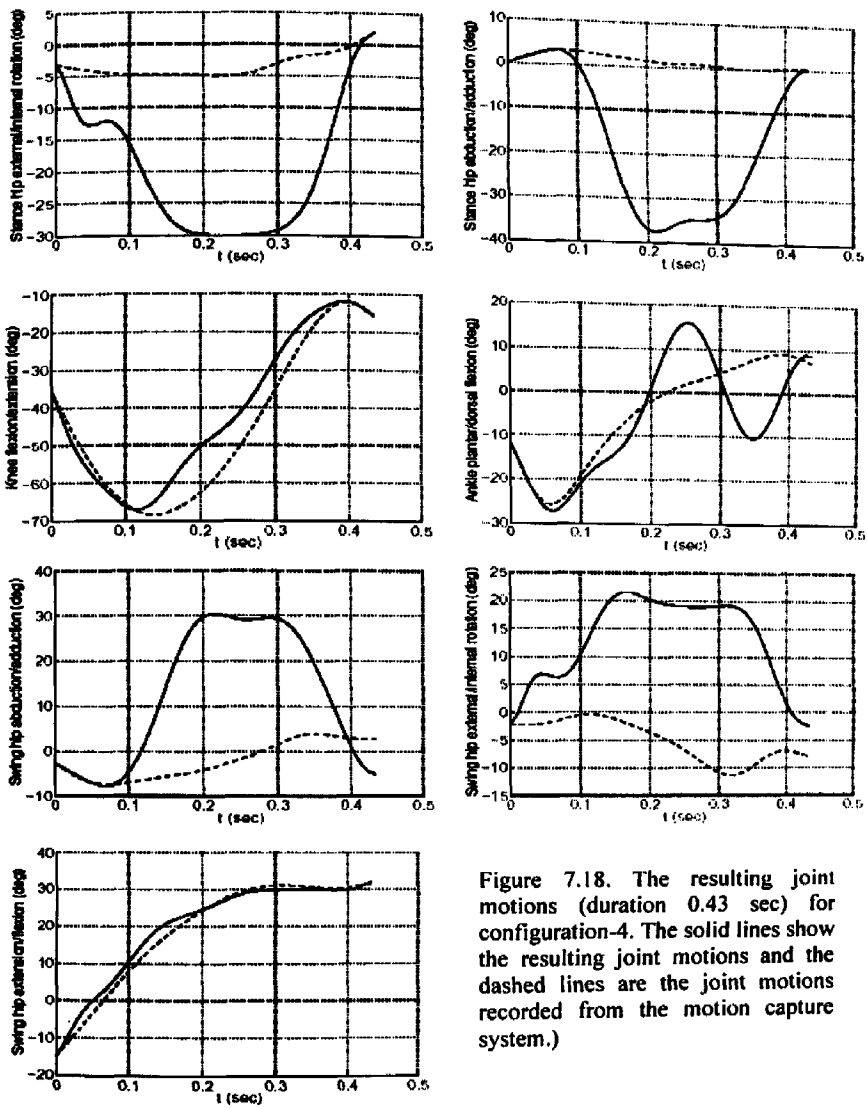


Figure 7.18. The resulting joint motions (duration 0.43 sec) for configuration-4. The solid lines show the resulting joint motions and the dashed lines are the joint motions recorded from the motion capture system.)

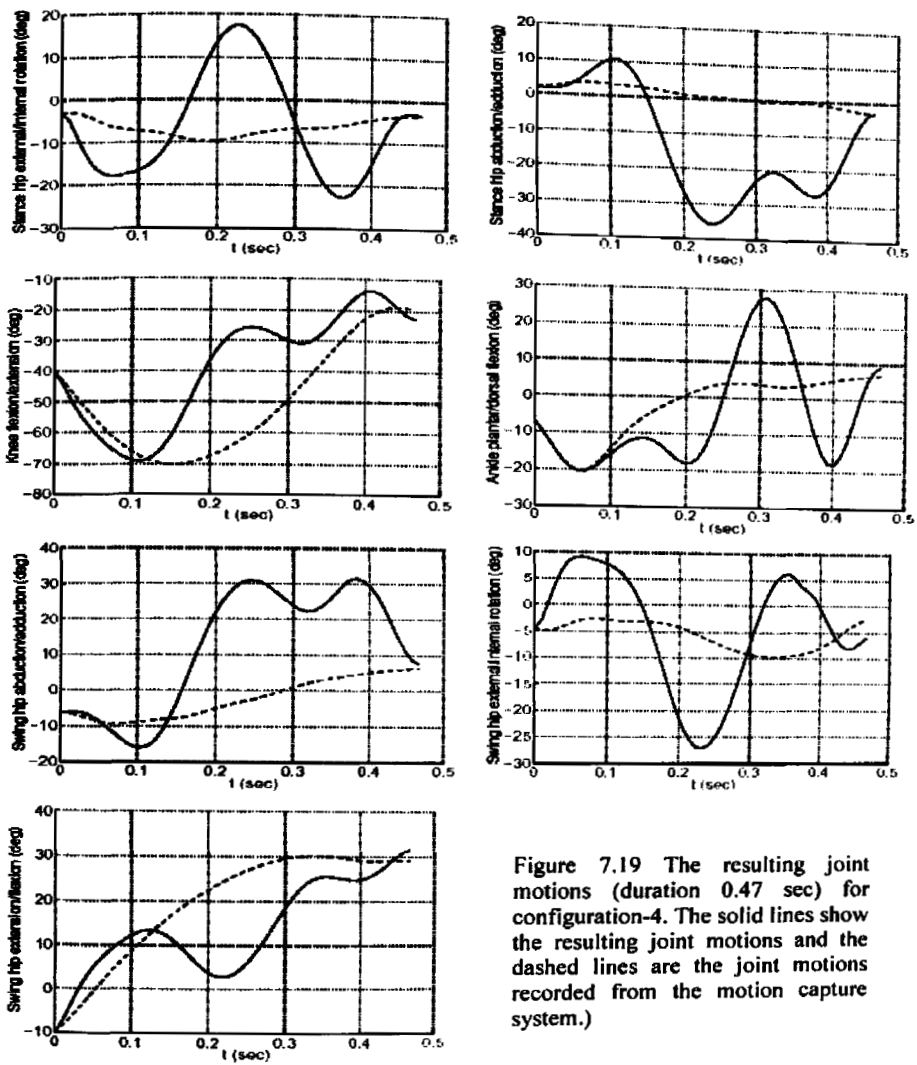


Figure 7.19 The resulting joint motions (duration 0.47 sec) for configuration-4. The solid lines show the resulting joint motions and the dashed lines are the joint motions recorded from the motion capture system.)

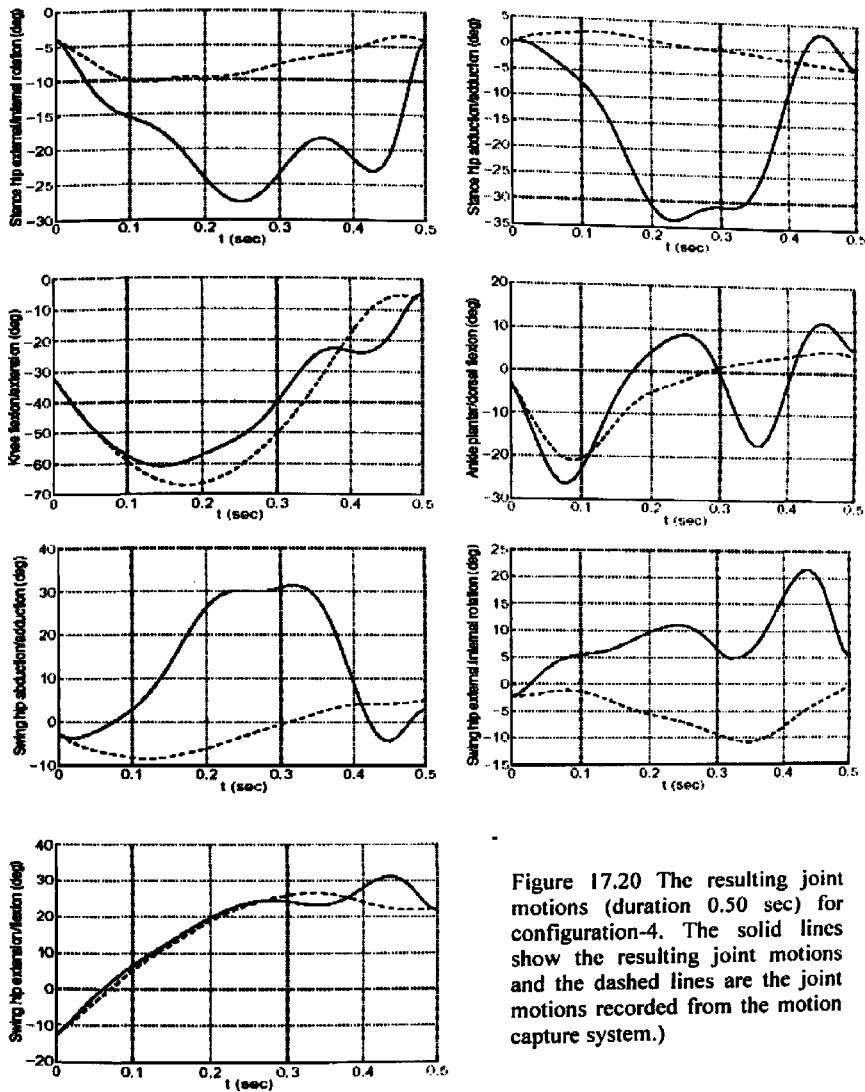


Figure 17.20 The resulting joint motions (duration 0.50 sec) for configuration-4. The solid lines show the resulting joint motions and the dashed lines are the joint motions recorded from the motion capture system.)

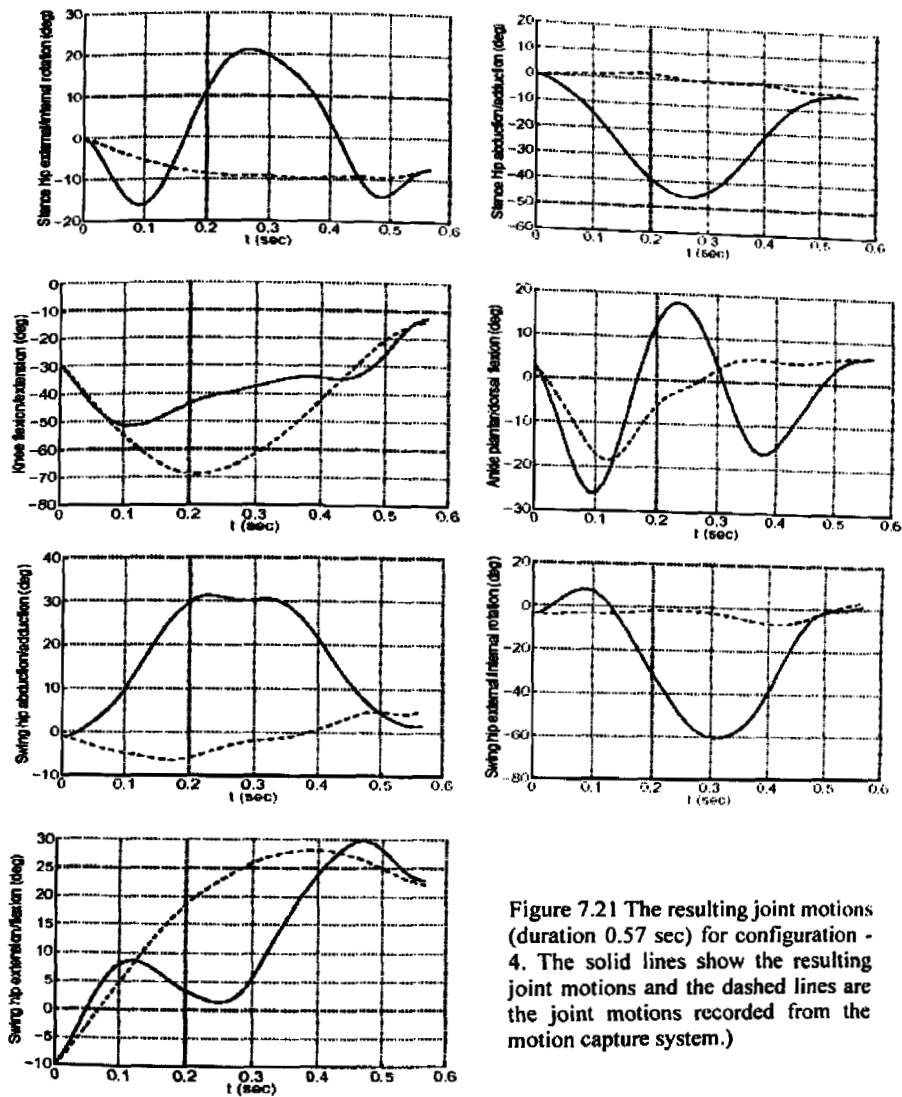


Figure 7.21 The resulting joint motions (duration 0.57 sec) for configuration - 4. The solid lines show the resulting joint motions and the dashed lines are the joint motions recorded from the motion capture system.)

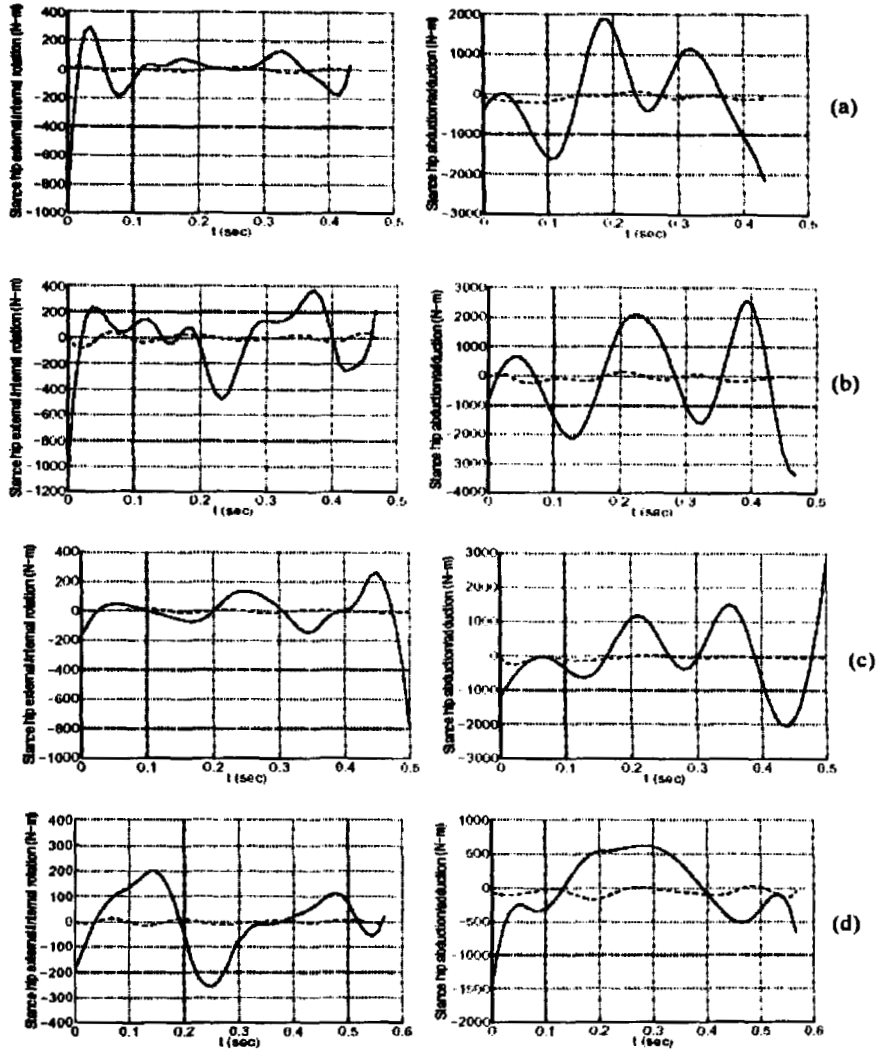


Figure 7.22 The resulting joint torques for configuration-4. The solid lines show the resulting joint torques and the dashed lines are the joint torques corresponding to the motion capture data). (a) duration 0.43 sec (b) duration 0.47 sec (c) duration 0.50 sec (d) duration 0.57 sec

7.5 PARALYZED SWING LEG WITH EFFORT MINIMIZATION OF THE STANCE HIP TORQUES AND BOUNDED STANCE HIP ORIENTATION (Configuration -4)

In order to determine if the large swivel motion in the previous configuration could be eliminated while still achieving a swing motion, the stance hip external/internal rotation within $\pm 30^\circ$ range was restricted by adding the following hard constraint to the optimization

$$-\frac{\pi}{6} \leq q_4 \leq \frac{\pi}{6}, \text{ or } -\frac{\pi}{6} \leq p_4 \leq \frac{\pi}{6} \quad (7.4)$$

The optimization took about 3 hours to complete. The results are shown in Figures 7.17 – 7.22, and demonstrate that a reasonable swing motion can be achieved while limiting excessive hip swivel.

7.6 COMPARISON OF CONFIGURATIONS

The applied effort, root-mean-square (RMS) of the position error (compared to the actual human gait), and norm of the final position error corresponding to different gait durations for different configurations are summarized in Figure 7.23, 7.24, and 7.25, respectively. Figure 7.23 demonstrates that most of the effort went into tilting the pelvis, i.e. abducting the stance hip, due to working against gravity. It also shows that the underactuated models in configuration 3 and 4 need close to the same amount of effort to shift the stance hip to complete a gait. From Figures 7.24 and 7.25, the fully actuated model in configuration 2 yields the best performance compared to the others. On one hand, the underactuated model in configuration 4 yields a smaller RMS error than that in configuration 3 because of the bound in its stance hip external/internal rotation. On the other hand, the bound limits the swivel of the pelvis which causes the underactuated model in configuration 4 to yield a larger final position error than that in configuration 3 for the faster movements.



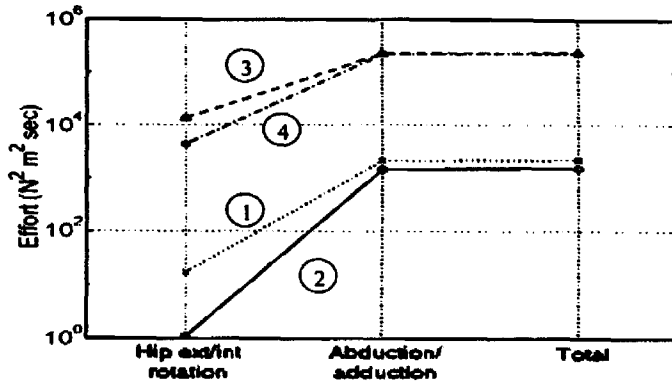


Figure 7.23 Applied effort for step duration 0.5 sec for configuration 1, 2, 3 and 4, respectively.

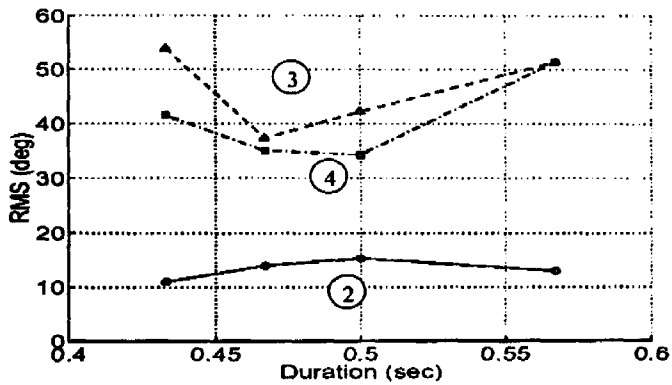


Figure 7.24 Root-Mean-Square of position error for the configuration 2, 3 and 4, respectively

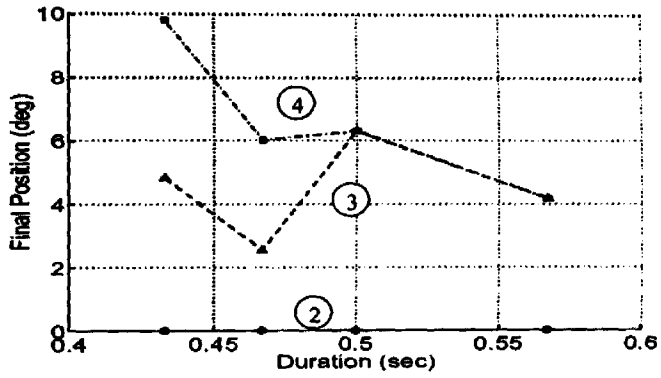


Figure 7.25 Final position error for the configuration 2, 3 and 4, respectively